NDT&E International 132 (2022) 102713

Contents lists available at ScienceDirect

NDT and E International

journal homepage: www.elsevier.com/locate/ndteint

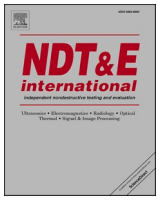

Improved thickness measurement on rough surfaces by using guided wave cut-off frequency

Sebastian Heinlein [a], Stefano Mariani [a], Josh Milewczyk [a], Thomas Vogt [a], Peter Cawley [a,b,*]

[a] Guided Ultrasonics Ltd, Brentford, TW8 8HQ, UK
[b] Imperial College, London, SW7 2AZ, UK

A B S T R A C T

Substantial variability is seen when thickness measurements using conventional ultrasonic time of flight measurements are carried out on rough surfaces; this makes it difficult to estimate corrosion rates when the corrosion mechanism leads to surface roughness. It has been shown that thickness measurements using guided wave cut-off frequencies (through thickness resonance frequencies) can be done at much lower frequencies than conventional time of flight thickness gauging for the same minimum thickness resolution. The lower frequency measurements are less susceptible to variations caused by surface roughness and so will give more consistent and reliable results in cases where corrosion leads to increased surface roughness. Measurements were carried out using guided wave cut-off frequencies on four plates with different surface roughness. On a plate with root mean square (rms) surface roughness of 0.3 mm, the thickness estimates followed the trend predicted from the plate geometry and probe footprint, whereas higher frequency measurements reported in the literature deviated from this trend at an rms roughness of 0.1 mm. The guided wave cut-offcut-off frequency measurements can be done using the same transduction system as that used for large area guided wave monitoring so it is possible to combine large and small area monitoring in a single unit. Frequent measurements enable the wall thickness obtained with guided wave cut-off measurements to be tracked with time, and the low susceptibility of the measurements to surface roughness means that accurate corrosion rates will be obtained.

1. Introduction

Ultrasonic thickness gauging typically involves a time-of-flight measurement, either between the front and back surface reflections from the testpiece, or successive back surface reflections [1]. If contact transduction without a significant delay line is used then the front surface reflection is not measured; in this case the excitation pulse applied to the transducer can be used as the time reference, with appropriate calibration to account for travel through the transducer structure. This is very straightforward on flat surfaces in the laboratory, and an accuracy of ±0.025 mm (±0.001 in) is commonly quoted [1]. However, much greater scatter in results is reported in field measurements [2]. For example, Yi et al. [3] and Lee et al. [4] show poor repeatability of up to ±0.3 mm (±0.012 in) and poor reliability, and some operators report large fractions of erroneous results [5]; the results also tend to be poorer in areas of changing geometry such as elbows, reducers and tees [4]. Wilson et al. [6] found that the 95% thickness confidence interval at some locations was as wide as ±1.1 mm.

Historically, this poor repeatability was ascribed to operator error due to repeat measurements not being taken at exactly the same location, or variations in the coupling layer between the transducer and the testpiece. However, when permanently installed thickness monitoring with frequent wireless transmission of thickness data became viable [7], thereby ensuring consistent position and coupling, it was found that sudden jumps in the computed thickness were sometimes seen, and that the thickness could appear to increase. This variability was particularly prevalent when the corrosion mechanism causing the wall loss tended to produce a rough surface, and it was shown [8] that the changes in thickness measurement in permanently installed systems were due to the varying topology of the back wall producing a change in shape of the ultrasonic signal; this could move the time-location of the peak of the signal, so making any method based on peak-peak timing particularly susceptible to variation. Jarvis and Cegla [8] showed that significant variation was seen with different possible algorithms and Wilson et al. [6] also showed that reliable thickness measurement was more difficult on rough surfaces.

Benstock et al. [9] showed that the uncertainty in thickness measurement produced by rough surfaces is a function of the ratio of the rms surface roughness to the ultrasonic wavelength (σ/λ) and becomes significant when the rms roughness exceeds about 10% of the wavelength. Gajdacsi and Cegla [10] showed that it is possible to mitigate the effect of roughness changes by using a novel adaptive cross correlation algorithm, but this involves tracking the signal with time and so the thickness obtained from a given signal is dependent on the preceding signals,

* Corresponding author. Guided Ultrasonics Ltd, Brentford, TW8 8HQ, UK.
E-mail address: p.cawley@imperial.ac.uk (P. Cawley).

https://doi.org/10.1016/j.ndteint.2022.102713
Received 14 June 2022; Received in revised form 29 July 2022; Accepted 30 July 2022
Available online 5 August 2022

which complicates the processing and data handling required.

The permanently installed system described by Cegla et al. [7] and commercialised by Permasense [11] uses a 5 cycle windowed toneburst to excite SH bulk waves at a frequency of 2 MHz, giving a central wavelength of ~1.6 mm; the results presented suggest that successive back face reflections from a 3 mm thick testpiece would be just resolvable, implying that thicknesses just under twice the central wavelength can be resolved.

The work of [9] suggests that the problem would be much reduced if the measurement could be taken at frequencies such that the σ/λ ratio is below 0.1. An alternative to ultrasonic time-of-flight measurements for thickness determination is to use through-thickness resonance frequency measurements; these frequencies correspond to the cut-off frequencies of the non-zero order guided wave modes. This has been known for many years and has been applied in different contexts [12–14]. The use of ultrasonic resonance frequency measurements for dimension or elastic modulus determination has become popularly known as resonant ultrasound spectroscopy [15] and Rus and Grosse [16] have pointed out that it is possible to measure the thickness of thinner plates than with time-of-flight measurements at a similar nominal frequency.

In the first through thickness resonance mode, the wavelength is double the plate thickness. If a 3 mm steel plate is to be measured and shear waves are to be used, as in Ref. [7], then the wavelength required is 6 mm, implying a frequency of around 500 kHz (given the shear wave speed of ~3250 m/s) rather than the 2 MHz required for the time-of-flight measurements of [7]. Benstock et al. [9] showed that with a 2 MHz time-of-flight system, accurate thicknesses can be obtained at an rms roughness of about 0.1 mm, implying that good results might be obtainable at rms roughnesses approaching 0.4 mm with a 500 kHz measurement. This paper investigates whether this can be achieved in practice using through thickness resonance frequency measurements with a commercial instrumentation system.

The paper is organised as follows: section 2 describes the measurement system used, while section 3 reports the results obtained on the specimens used previously in the investigation of [9]. Finite element predictions of the results of section 3 are presented in section 4, followed by example field results in section 5 and the conclusions of the study in section 6.

2. Practical measurement system

Fig. 1a shows a guided wave permanently installed monitoring system (gPIMS) produced by Guided Ultrasonics Ltd [17]. It comprises two rows of piezoelectric elements, the assembly being over-moulded in polyurethane to provide environmental protection. The assembly is bonded to the test pipe and connected to instrumentation that can either be permanently installed to carry out the test and send the resulting data wirelessly to the control room, or can be operated via plug-in instrumentation if only occasional testing is required. The piezoelectric elements are shear polarised and are designed to exert a force in the circumferential direction on the pipe; they are spaced approximately 25 mm apart in the circumferential direction and 32 mm apart in the axial direction so the number of elements increases with the pipe diameter. This arrangement was originally designed for guided wave testing; if all the transducer elements in one row are excited together then a torsional wave is excited in both directions along the pipe, and by appropriate phasing of the excitation to the second row, the wave can be transmitted either to the left or right along the pipe [18]. Returning echoes from features in the pipe are received by the same transducers and can be processed to produce an A-scan signal showing features along the pipe over a test range of 10s of metres.

Guided wave testing is done in the 10s of kHz frequency range, but

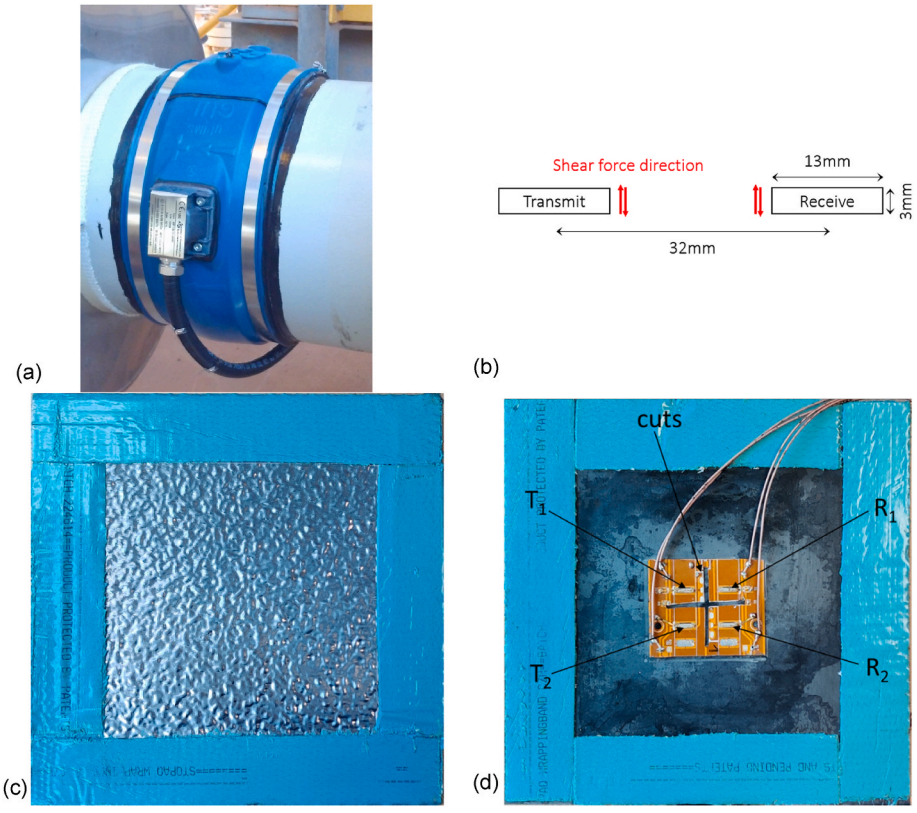

Fig. 1. (a) Full gPIMS (permanently installed monitoring system) on 8 inch pipe; (b) schematic diagram of pair of piezoelectric elements with centre-centre spacing 32 mm showing direction of forcing; (c) rough side of plate with 0.3 mm rms roughness and Stopaq covering edges outside rough area; (d) system of (b) coupled to plain side of test plate with Stopaq around edges showing two pairs of transmitters (T_i) and receivers (R_i) and cuts in the PCB to block transmission solely in the board.

the piezoelectric elements can also be driven at higher frequencies so it was realised that the same transduction system could be used for thickness resonance testing; this has been patented [19]. A pair of transducers corresponding to one piezoelectric element from each of the two rows is shown schematically in Fig. 1b. If the assembly is mounted on a plate or pipe and one of the elements is excited with a windowed toneburst containing energy at the thickness resonance frequency, the resulting through-thickness ringing will be detected by the second transducer and the resulting signal can be processed to give the resonance frequency and hence the thickness, given the speed of sound. The speed of sound can either be assumed from material data or can be measured from the arrival time difference of torsional guided wave reflections from features a known distance apart when the system is used in guided wave mode. These measurements can also enable compensation of the thickness readings for speed of sound changes with temperature. Pitch-catch measurements between transmitting and receiving transducers are used rather than pulse echo measurements at a single transducer because the reverberations in the plate that give the thickness would be swamped by reverberations in a single transducer following the excitation pulse.

Fig. 1d shows two transducer pairs of the type shown schematically in Fig. 1b mounted on an 8 mm thick steel plate with a rough surface machined on the reverse side as shown in Fig. 1c. The piezoelectric elements are mounted on a flexible printed circuit board (PCB) to facilitate the electrical connections and the board is cut in between the transducers to prevent the reception of waves travelling solely in the PCB. The piezoelectric elements are 1 mm thick and in this experiment are shear-polarised PZT-5A; the type of PZT is not critical and could be varied if required by the operational conditions. In this instance the transducer assembly was coupled via treacle (a very viscous substance similar to honey) rather than adhesive so that there was satisfactory shear coupling into the plate and the transducer could be moved to other locations/plates for further tests; during measurements the transducer was also pressed onto the pipe with a G-clamp (not shown in Fig. 1d for clarity). Fig. 2a shows the signal received by the receiving transducer when the transmitter was excited with a 220 kHz Hann windowed toneburst, the signals being generated and received by a Guided Ultrasonics Ltd Wavemaker G4-Mini instrument. The initial signal is breakthrough from the excitation pulse combined with the SH0 wave travelling between the transmitter and receiver; this is followed by a ringing signal corresponding to the through-thickness reverberations. Fig. 2b shows the reverberations on an expanded scale after gating out the initial signal and the signal after 0.5 ms; Fig. 2c shows the spectrum of the signal of Fig. 2b obtained via Fourier transformation, together with the spectrum of the input signal. The input signal is much broader band than the response so the peak of the response is a good approximation to the peak of the transfer function between response and input. The peak corresponds to the first through thickness shear mode of the plate; this frequency also corresponds to the cut-off frequency of the SH1 guided wave mode as shown in Fig. 3 (the frequency is not exactly the same since nominal properties were used to calculate the dispersion curves). The thickness, t, can simply be obtained from:

$$t = \frac{nc_s}{2f_n} \tag{1}$$

where c_s is the shear wave speed (taken as 3250 m/s here) and f_n is the frequency of mode n; only mode 1 was used in the tests reported here. Since the transmitting and receiving transducers are a short distance apart, there is some transmission along the plate so the frequency measured is not strictly the cut-off. However, the response is strongly dominated by modes propagating close to the cut-off frequency. The error in taking it as the cut-off was found to be negligible and, since the distance is unchanged in successive readings, it has no effect on thickness loss estimates. The transmission of reverberations along the plate between the transmitter and receiver can also be viewed as a diffraction phenomenon: since the transducers are small and the wavelength is long, there is considerable beam spreading so the reverberations between the top and bottom surfaces of the plate are not confined to the region of the transmitter but spread along the plate with each reverberation.

Tests were carried out on four square 8 mm thick steel plates with 300 mm side length. The first plate was flat while the others had one side machined to 0.1, 0.2 and 0.3 mm rms surface roughnesses using a CNC milling machine. The plates were machined using the same input data file as used to produce the specimens of [9], the rough surface being produced over the central square region with 200 mm side length. The correlation length of the roughness on each of the rough plates was 2

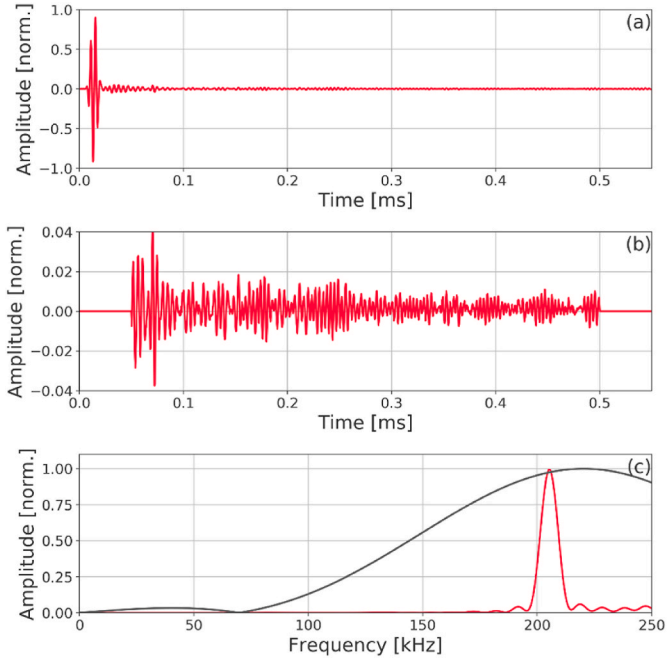

Fig. 2. (a) Received signal on plain plate. The large initial signal (pre ~0.05 ms) is breakthrough from the excitation pulse coupled with the SH0 mode travelling from the transmitter to the receiver; (b) reverberations corresponding to through thickness resonance gated from signal of (a) on enlarged scale; (c) spectrum of (b) in red with spectrum of input signal in black. (For interpretation of the references to colour in this figure legend, the reader is referred to the Web version of this article.)

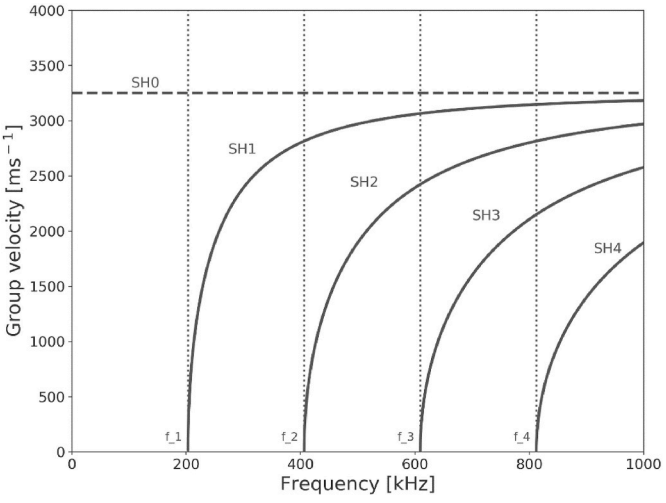

Fig. 3. Group velocity dispersion curves for SH waves in 8 mm thick steel plate. SHi denote the modes; f_i at the bottom of the curves show the corresponding cut-off frequencies.

mm as in Ref. [9]. The regions outside the rough area were coated with Stopaq [20,21] in order to damp guided wave reflections from the plate edges that would not be present in a typical installation on a long pipe; the corresponding region of the flat plate was coated in the same way. The coating can be seen in Fig. 1(c) and (d).

Initial tests investigated the reproducibility of the results by coupling the transducer to the plain plate at the same location 42 times. The standard deviation of the thickness obtained was 0.0066 mm; this random variability would not be seen if the transducer was permanently installed as the coupling would be consistent. Tests were then done at different locations on each plate in a rough grid pattern, the centre of the transducer assembly being a minimum of ~20 mm from the edge of the machined area on the rough plates; similar locations were tested on the plain plate. At least 30 measurements were done on each plate.

The temperature was roughly constant during the tests so temperature compensation was not required. If necessary the results could easily be compensated for temperature using the variation in shear velocity with temperature [7].

3. Lab test results

Fig. 4 shows the standard deviations of the measurements obtained at different locations on the four test plates, together with the results obtained by Benstock et al. [9] on similar plates using higher frequency time-of-flight measurements. Three different possible algorithms, time of first arrival (TFA), time between successive envelope peaks (EP) and cross correlation (XC) were investigated in Ref. [9], the standard deviation of the measurements generally being lowest with the TFA algorithm. Fig. 4 shows that the standard deviations of the results with the lower frequency resonance technique of this paper are substantially smaller than those obtained with any of the algorithms in the higher frequency time-of-flight measurements of [9]. Both methods effectively average the thickness over the probe footprint and this would be expected to reduce the standard deviation of the thicknesses measured at different transducer positions. The grey dashed line in Fig. 4 reproduces from Ref. [9] the estimate of the standard deviation of the mean thickness of the plates over an area corresponding to the high frequency probe footprint; the results obtained with all three algorithms show significantly more scatter than this, indicating that the high frequency measurements give more scatter than would be expected from the plate geometry and probe footprint; this is explained in Ref. [9].

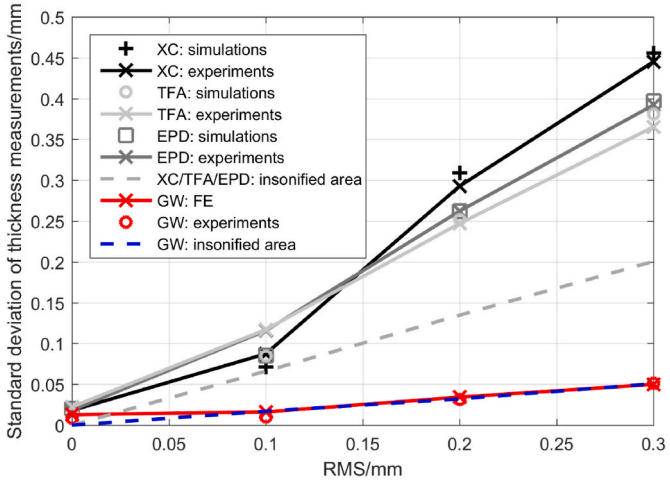

Fig. 4. Predicted and measured standard deviations of the measured thicknesses on plates with different surface roughness using the resonance method of this paper (colour) and the high frequency time of flight method (black/grey) with different algorithms from Ref. [9]. (For interpretation of the references to colour in this figure legend, the reader is referred to the Web version of this article.)

The effective footprint of the probe used in this investigation, A, can be considered to be the ellipse corresponding to the first Fresnel zone with the transmitting and receiving transducers at its foci [22].

$$A = \frac{\pi}{4}\sqrt{\lambda L^3} \tag{2}$$

where L is the distance between the transducers and the wavelength, λ, in the first through thickness mode is twice the plate thickness. This area is larger than that for the high frequency probe of [9] so the standard deviation of the mean thickness of the plates over this footprint shown in the blue dashed line of Fig. 4 is smaller than that given by the grey dashed line. The experimental results shown in red circles are very close to this line, indicating that the low frequency method proposed in this paper gives similar scatter in results to that expected from the plate geometry and probe footprint. It is therefore more accurate than the higher frequency methods, as was hypothesised in the introduction to this paper.

4. FE modelling

Finite element 3D models of the four plates and of the transduction system used in the lab tests were generated in Pogo [23]. The same input data files used to machine the plates were used to create exact replicas of the actual rough patches. For example, Fig. 5 shows the plate at 0.3 mm rms surface roughness. Steel was modelled as an isotropic medium with density of 8000 kg/m^3, an elastic modulus of 216.9 GPa and a Poisson's ratio of 0.2865, which gives shear and longitudinal velocities of 3250 m/s and 5940 m/s respectively. Each plate was discretised via linear hexahedral elements with sides of ~0.5 mm, for a total of 7.2 M elements. The chosen mesh size provides about 30 elements per wavelength of the first through thickness shear resonance of the plate (wavelength twice the plate thickness), hence safely meeting the most stringent accuracy requirements for elastodynamic simulations [24]. To ensure stability, the Courant-Friedrichs-Lewy condition dictates that the fastest wave must not travel through more than one element in a single time-step [25]. By setting the simulation time-step to 10 ns, longitudinal waves require more than 8 time-steps to travel across a single element, hence safely satisfying the stability requirement.

The excitation stage of the transmitter was modelled by applying a shear force to the nodes found within the footprint of the piezoelectric element surface, in the direction shown in Fig. 1b. Similarly, the wave sensing stage was simulated by summing up the predicted displacements in the forcing direction at the nodes within the footprint of the receiving transducer. Absorbing boundaries were assigned to the regions of the plates outside the machined area using the standard formulation available in Pogo [26].

Simulations were conducted on each plate as the pair of transducers was moved in a 2D raster pattern at 5 mm steps across the inner 200 × 200 mm region (where the rough surfaces are located). As in the experiments, the excitation signal was a 3 cycle, Hann windowed 220 kHz

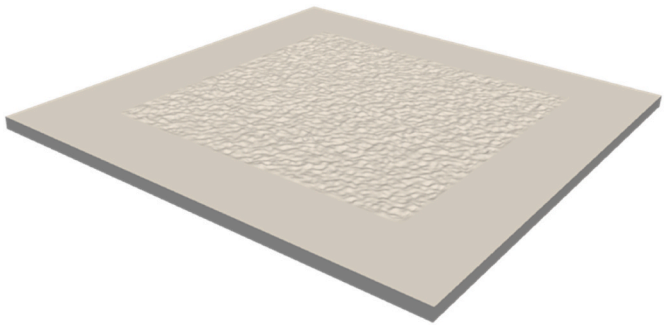

Fig. 5. Modelled plate with 0.3 mm rms roughness. The side length is 300 mm with the rough surface over the middle 200 mm.

toneburst and the signal at the receiver was predicted over a length of 50,000 time-steps, which corresponds to ~0.5 ms. The predicted signals were processed using the same algorithm as used for the experimental data.

The predicted results are shown in the red line of Fig. 4. This agrees very well with the experimental results and also closely follows the standard deviation of the thickness of the plate over the effective probe footprint. Some scatter in results is predicted even in the zero roughness case; this is a result of guided wave reflections from the plate edges that are not completely suppressed by the absorbing boundaries. Good absorption performance is usually obtained when such boundaries are longer than three times the incoming wavelengths [26]. The employed length of 50 mm offers about 4 wavelengths in the A0 mode at the excitation frequency of 220 kHz, but only 2 wavelengths to the S0 mode, hence some edge reflections are still reverberating within the plate. This is also seen in the experiments where the Stopaq coating does not completely suppress the edge reflections.

5. Example field results

5.1. Comparison of phased array and guided wave thickness measurements

Fig. 6a shows one of a series of PIMS installations on a 36 inch buried line that was known to be corroded, the gPIMS moulding being green in this instance rather than the ATEX-certified blue system of Fig. 1a. Phased array ultrasonic thickness (PAUT) measurements at the location of each gPIMS were taken before the installation, an example C-scan thickness map being shown in Fig. 6b. Significant thickness variation is evident; the guided wave system comprises 108 transducer pairs around

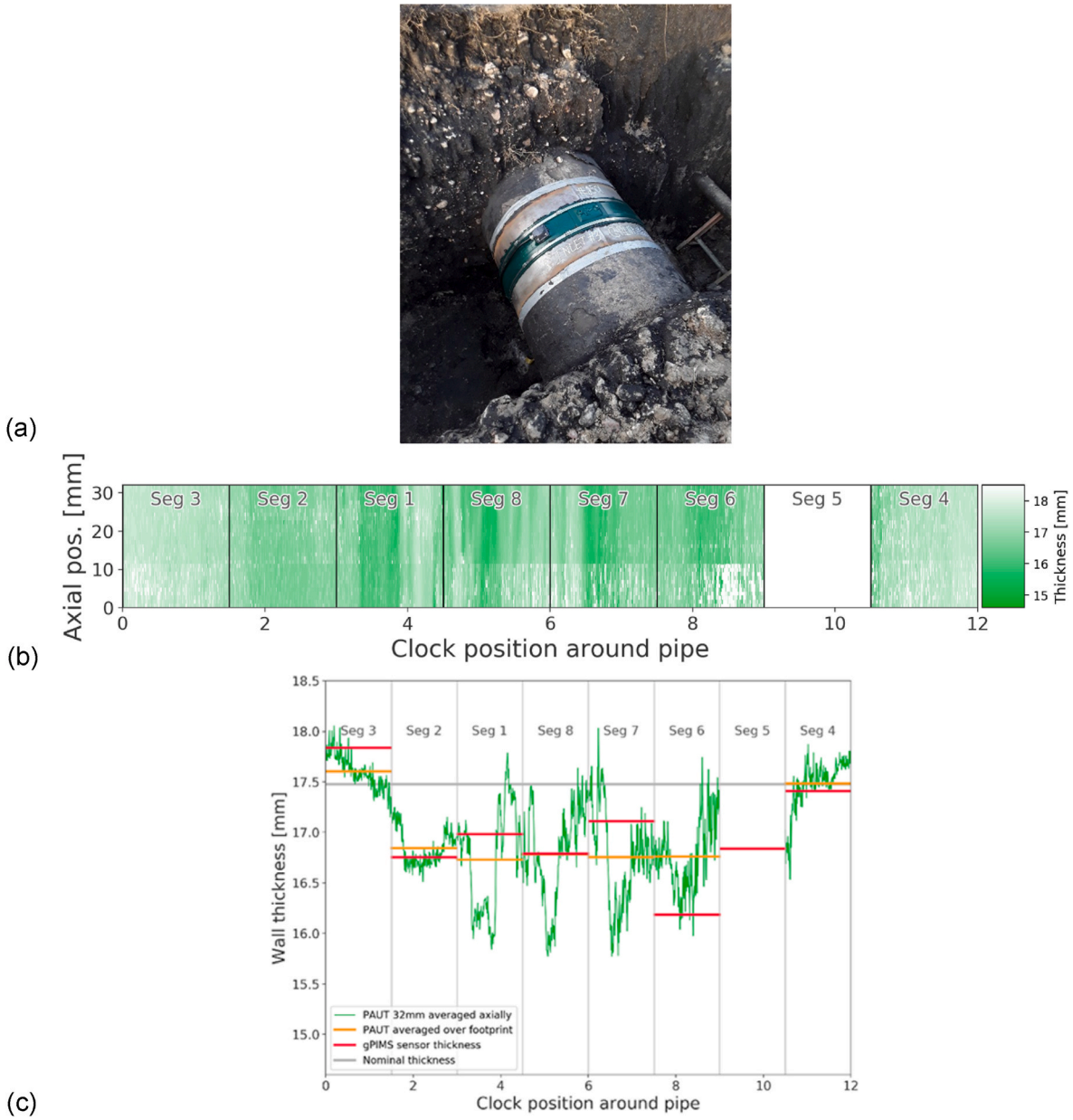

Fig. 6. Tests on 36 inch diameter pipe in the field. (a) Photograph of installation. Here the permanently installed sensor (gPIMS) is green rather than the ATEX-certified, blue, unit of Fig. 1a; (b) C-scan of phased ultrasonic array (PAUT) thickness estimate taken before gPIMS installed; (c) comparison of PAUT results averaged over guided wave sensor footprint and guided wave based thickness measurements; the green line shows the PAUT thickness averaged in the axial direction showing how the thickness varies in the circumferential direction. (For interpretation of the references to colour in this figure legend, the reader is referred to the Web version of this article.)

the pipe circumference and these are divided into eight segments, four of which each have 13 transmitters and 13 receivers, and four have 14 of each. These sets of transmitters and receivers in a segment form one transmission and one receiver channel so the measured thickness is effectively averaged over the segment; this economises on wiring at a cost of spatial resolution. PAUT measurements were not taken over segment 5 as indicated on Fig. 6b. The continuous green line in Fig. 6c shows the PAUT thickness averaged in the axial direction as a function of circumferential position and so shows the variation in thickness with circumferential position over each segment. The mean PAUT thickness estimate over each segment and the guided wave thickness estimates are also shown, the two estimates agreeing to better than 0.5 mm compared to the nominal uncorroded thickness of 17.5 mm. Given the extent of variation over the surface, this agreement is very encouraging. The corroded pipe surface is rough so the PAUT measurements are subject to the thickness estimate errors discussed in Ref. [9] and should not be assumed to be 'true gold standard' values.

5.2. Stability with time

In most applications, the absolute thickness is less important than the corrosion rate. Operators want to know the range within which the corrosion rate, b, lies at a given level of confidence (b is in the range $b \pm \Delta b$ with eg 95% confidence). It may readily be shown from standard statistics [27] that Δb obtained from a sequence of N thickness readings taken over a time T is given by

$$\Delta b = \frac{\sigma P \sqrt{12}}{T\sqrt{N}} \tag{3}$$

where σ is the standard deviation of the thickness estimates and P is a constant depending on the confidence level required ($P = 1.96$ for 95% confidence). Therefore the uncertainty in corrosion rate is proportional to the standard deviation of the individual thickness measurements and is reduced by frequent readings over a longer period. Permanently installed installations facilitate frequent readings that are guaranteed to be at the same location and so enable much more accurate corrosion rate estimates than periodic manual spot thickness measurements. Fig. 7 shows a sequence of thickness readings from a field installation of a guided wave gPIMS system on a 12 inch diameter pipe with 47.5 mm nominal wall thickness. As might be expected, the eight segments show slightly different thicknesses, but all are stable over the ~6 months of data shown. The channel shown in brown has the largest standard deviation in readings but even this is only 0.02 mm, the others being 0.007 mm or below; the precision of the thickness measurements is therefore very good. Thus, from equation (3), on seven of the eight channels, one reading per day over a period of one month is sufficient to give an uncertainty in corrosion rate of ±0.1 mm/year or better, and this can be achieved over a period of one week if the data rate is increased to 4 collections per hour. It is therefore possible to obtain accurate corrosion rate information rapidly and so to, for example, track the impact of employing different feedstocks on plant life. This enables optimisation of the use of expensive corrosion inhibitor chemicals and provides the ability to process cheaper, more corrosive feedstocks while maintaining confidence in plant integrity. On the more noisy channel, an increase in data rate to 10 per day over a period of one month is sufficient to achieve an uncertainty of better than ±0.1 mm/year.

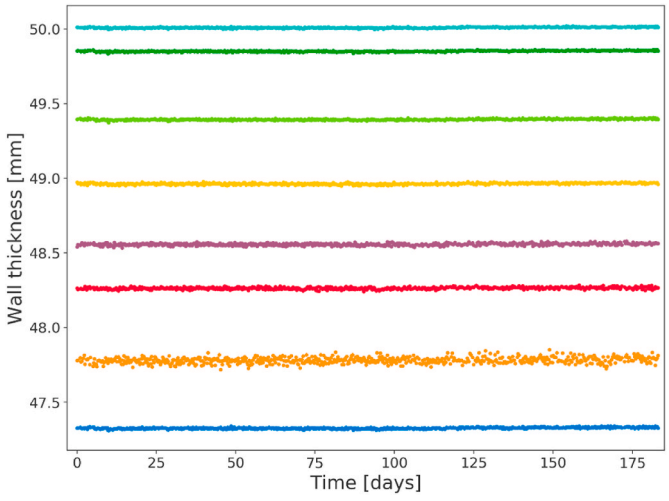

Fig. 7. Thickness readings taken over a period of ~6 months on the eight segments of a field installation on a 12 inch pipe with a nominal wall thickness of 47.5 mm.

6. Conclusions

It has been shown that thickness measurements using guided wave cut-off frequencies (through thickness resonance frequencies) can be done at much lower frequencies than conventional time of flight thickness gauging for the same minimum thickness resolution. The lower frequency measurements are less susceptible to variations caused by surface roughness and so will give more consistent and reliable results in cases where corrosion leads to increased surface roughness. Measurements were carried out using guided wave cut-off frequencies on four plates with different surface roughness. On a plate with root mean square (rms) surface roughness of 0.3 mm, the thickness estimates followed the trend predicted from the plate geometry and probe footprint, whereas higher frequency measurements reported in the literature deviated from this trend at an rms roughness of 0.1 mm.

Estimating the rate of corrosion induced wall loss with higher frequency measurements involves complicated tracking of the signal with time [10] so the results from a current test cannot be computed reliably without reference to previous signals, and the estimated thickness from the current test may affect estimates from earlier tests. This complication is removed with the lower frequency guided wave cut-off measurements proposed here. If the rms surface roughness were to increase to ~0.5 mm or more then some uncertainty in the lower frequency results would be seen, but at these very high roughnesses, the concept of a point thickness measurement becomes questionable.

The guided wave cut-off frequency measurements can be done using the same transduction system as that used for large area guided wave monitoring [18] so it is possible to combine large and small area monitoring in a single unit. The large area guided wave monitoring typically has a dead zone at the transducer ring location but this can now be covered by the local thickness measurement. Uniform wall loss over the whole pipe is typically difficult to detect using large area guided wave monitoring but this is very straightforward to detect with the small area thickness measurement. Conversely, localised wall loss at one location in a large area is difficult to detect with small area monitoring as it is likely that the transducer will not be placed at the exact location of the problem; this case is very well covered by large area guided wave monitoring so the two methods are complementary.

Frequent measurements enable the wall thickness obtained with guided wave cut-off measurements to be tracked with time, and the low susceptibility of the measurements to surface roughness means that accurate corrosion rates will be obtained.

Author contributions statement

Conception or design of the work – Vogt, Milewczyk, Data collection - Heinlein, Milewczyk, Mariani, Data analysis and interpretation – Heinlein, Milewczyk, Mariani, Drafting the article - Cawley, Critical revision of the article – Cawley, Vogt, Final approval of the version to be published - Cawley.

Declaration of competing interest

The authors declare the following financial interests/personal relationships which may be considered as potential competing interests: Peter Cawley reports a relationship with Guided Ultrasonics Ltd that includes: board membership and equity or stocks. Sebastian Heinlein reports a relationship with Guided Ultrasonics Ltd that includes: employment. Thomas Vogt reports a relationship with Guided Ultrasonics Ltd that includes: employment. Stefano Mariani reports a relationship with Guided Ultrasonics Ltd that includes: employment. Josh Milewczwyk reports a relationship with Guided Ultrasonics Ltd that includes: employment. Thomas Vogt, Josh Milewczyk has patent pending to Guided Ultrasonics Ltd.

Acknowledgements

The authors are grateful to Dr Frederic Cegla of Imperial College for providing the input files required to machine the rough plate specimens to the same specification as used in Ref. [9] and to Professor Peter Nagy for helpful discussions about the effective footprint of the guided wave probe and the Fresnel zone. They are also grateful to Jon Lorg, Ronnie Summerlin, and Scott Taylor of the Versa Integrity Group for allowing use of the phased array data of Fig. 6.

References

[1] Elder JB, Vande Kamp RW. Benefits of the multiple echo contact technique for ultrasonic thickness testing. Mater Eval 2011;69:1269–76.
[2] Cegla F, Allin J. Wireless ultrasonic thickness monitoring at elevated temperatures. Mater Eval 2001;69:A27–31.
[3] Yi WG, Lee MR, Lee JH, Lee SH. A study on the ultrasonic thickness measurement of wall thinned pipe in nuclear power plants. In: 12th Asia-Pacific conference on NDT; 2006. Auckland, New Zealand.
[4] Lee D-H, Lee S-J, Lee J-H, Lee S-H. Analysis of round robin test for ultrasonic thickness measurement of wall thineed pipe in nuclear power plant. AIP Conf Proc 2008;975:1732–8.
[5] van Roodselaar A, Huyse L, Hsiao CP, Seiwald M. Statistical modeling of some NDE measurement uncertainties. In: Inspector summit conference Proceedings. Texas: Galveston; 2009.
[6] Wilson PT, Krouse DP, Moss CJ. Statistical Analysis of UT Wall thickness data from corroded plant. Non-destructive Testing Australia 2004;41:77–84.
[7] Cegla FB, Cawley P, Allin J, Davies J. High-temperature (>500°C) wall thickness monitoring using dry-coupled ultrasonic waveguide transducers. IEEE Trans Ultrason Ferroelectrics Freq Control 2011;58:156–67.
[8] Jarvis AJ, Cegla FB. Application of the distributed point source method to rough surface scattering and ultrasonic wall thickness measurement. J Acoust Soc Am 2012;132:1325–35.
[9] Benstock D, Cegla FB, Stone M. The influence of surface roughness on ultrasonic thickness measurements. J Acoust Soc Am 2014;136:3028–39.
[10] Gajdacsi A, Cegla FB. The effect of corrosion induced surface morphology changes on ultrasonically monitored corrosion rates. Smart Matreials and Structures 2016; 25:115010.
[11] Permasense Ltd. now part of Emerson Inc, [Online], www.permasense.com.
[12] J.-C. Carossi and P. Fierard, "Method and device for the measurement of thickness by ultrasonic resonance," US patent 3,844,166, 1974.
[13] Dixon S, Lanyon B, Rowlands G. Coating thickness and elastic modulus measurement using ultrasonic bulk wave resonance. Appl Phys Lett 2006;88: 141907.
[14] Urayama R, Takagi T, Uchimoto T, Kanemoto S, Ohira T, Kikuchi T. Implementation of electromagnetic acoustic resonance in pipe inspection. J Adv Maintain 2013;5:25–33. Japan Society of Maintenology.
[15] Balakirev FF, Ennaceur SM, Migliori RJ, Maiorov B, Migliori A. Resonant ultrasound spectroscopy: the essential toolbox. Rev Sci Instrum 2019;90:121401.
[16] Rus J, Grosse CU. Thickness measurement via local ultrasonic resonance spectroscopy. Ultrasonics 2021;109:106261.
[17] Guided Ultrasonics Ltd [Online], http://www.guided-ultrasonics.com.
[18] Alleyne DN, Pavlakovic B, Lowe MJ, Cawley P. Rapid long-range inspection of chemical plant pipework using guided waves. Insight 2001;43(101):93–6.
[19] Vine K, Vogt T, Milewczyk SJ. Methods and systems for determining a thickness of an elongate or extended structure". Priority GB201816552A Patent WO2020074895A1; 2018.
[20] Bessant A. Putting an end to coating disbondment: viscous-elastic coatings for transportation pipelines, vol. 87. Corrosion Management; 2009. p. 15–8.
[21] Huthwaite P, Ribichini R, Cawley P, Lowe MJ. Mode selection for corrosion detection in pipes and vessels via guided wave tomography. IEEE Trans Ultrason Ferroelectrics Freq Control 2013;60:1165–77.
[22] Fei H, Xiao F, Huang H, Sun L. Indoor static localization based on Fresnel zones model using COTS Wi-Fi. J Netw Comput Appl 2020;167:102709.
[23] Huthwaite P. Accelerated finite element elastodynamic simulations using the GPU. J Comput Phys 2014;257:687–707.
[24] Moser F, Jacobs L, Qu J. Modeling elastic wave propagation in waveguides with the finite element method. NDT&E International 1999;32:225–34.
[25] Courant R, Friedrichs K, Lewy H. On the partial difference equations of mathematical physics. IBM Journal 1967;11:215–34.
[26] Petit JR, Walker A, Cawley P, Lowe MJ. A stiffness reduction method for efficient absorption of waves at boundaries for use in commercial finite element codes. Ultrasonics 2014;54:1868–79.
[27] Bulmer MG. Principles of statistics. New York: Dover; 1979.